IOP Publishing Physiol. Meas. 40 (2019) 025007 (15pp) https://doi.org/10.1088/1361-6579/ab009b

Physiological Measurement

IPEM Institute of Physics and Engineering in Medicine

RECEIVED
12 October 2018

REVISED
10 January 2019

ACCEPTED FOR PUBLICATION
22 January 2019

PUBLISHED
25 February 2019

PAPER

Optimal fiducial points for pulse rate variability analysis from forehead and finger photoplethysmographic signals

Elena Peralta[1,2], Jesus Lazaro[1,2,4], Raquel Bailon[1,2], Vaidotas Marozas[3] and Eduardo Gil[1,2]

[1] Biomedical Signal Interpretation and Computational Simulation (BSICoS) Group, Aragon Institute of Engineering Research (I3A), IIS Aragon, University of Zaragoza, Zaragoza, Spain
[2] Centro de Investigacion Biomedica en Red—Bioingenieria, Biomateriales y Nanomedicina (CIBER-BBN), Zaragoza, Spain
[3] Biomedical Engineering Institute and Electronics Engineering Department, Kaunas University of Technology, Kaunas, Lithuania
[4] Department of Biomedical Engineering, University of Connecticut, Storrs, CT, United States of America

E-mail: elena.peralta.calvo@gmail.com

Keywords: photoplethysmography (PPG), ECG, heart rate variability, pulse rate variability, autonomic nervous system, fiducial point selection, transmission and reflection modes

Abstract

Objective: The aim of this work is to evaluate and compare five fiducial points for the temporal location of each pulse wave from forehead and finger photoplethysmographic (PPG) pulse wave signals to perform pulse rate variability (PRV) analysis as a surrogate for heart rate variability (HRV) analysis. *Approach*: Forehead and finger PPG signals were recorded during a tilt-table test simultaneously with the electrocardiogram (ECG). Artefacts were detected and removed and five fiducial points were computed: apex, middle-amplitude and foot points of the PPG signal, apex point of the first derivative signal and the intersection point of the tangent to the PPG waveform at the apex of the derivative PPG signal and the tangent to the foot of the PPG pulse, defined as the intersecting tangents method. Pulse period (PP) time interval series were obtained from both PPG signals and compared with the RR intervals obtained from the ECG. HRV and PRV signals were estimated and classical time and frequency domain indices were computed. *Main results*: The middle-amplitude point of the PPG signal (n_M), the apex point of the first derivative (n_A^*), and the tangent intersection point (n_T) are the most suitable fiducial points for PRV analysis, resulting in the lowest relative errors estimated between PRV and HRV indices and higher correlation coefficients and reliability indices. Statistically significant differences according to the Wilcoxon test between PRV and HRV signals were found for the apex and foot fiducial points of the PPG, as well as the lowest agreement between RR and PP series according to Bland–Altman analysis. Hence, these signals have been considered less accurate for variability analysis. In addition, the relative errors are significantly lower for n_M and n_A^* using Friedman statistics with a Bonferroni multiple-comparison test, and we propose that n_M is the most accurate fiducial point. Based on our results, forehead PPG seems to provide more reliable information for a PRV assessment than finger PPG. *Significance*: The accuracy of the pulse wave detection depends on the morphology of the PPG. There is therefore a need to widely define the most accurate fiducial point for performing a PRV analysis under non-stationary conditions based on different PPG sensor locations and signal acquisition techniques.

1. Introduction

Heart rate variability (HRV) analysis is a non-invasive technique for evaluation of the autonomic nervous system (ANS) (TaskForce 1996) based on the electrocardiogram (ECG) recording. This signal is normally measured using two or more electrodes placed at various positions on the chest and/or limbs. An alternative approach is to estimate pulse rate variability (PRV) from the pulse photoplethysmographic (PPG) signal by simply measuring the changes in blood flow as changes in the intensity of the light reflected or transmitted through the tissues. The PPG signal is a particularly interesting, simple, low-cost, reliable and comfortable technique for the estimation of heart rate (Bernardi *et al* 1997, Niztan *et al* 1998, Allen *et al* 2007), and the signal only needs to be acquired from

© 2019 Institute of Physics and Engineering in Medicine

a single location on the body. The main differences between PRV and HRV are due to physiological factors and to the variability of the location of the PPG fiducial point (Gil *et al* 2010). These physiological factors include pulse transit time (PTT), which is the time the pulse wave takes to travel from the heart to the periphery, and the pre-ejection period (PEP), a small delay between ventricular depolarization and the opening of the aortic valve, also known as the isovolumic contraction time. Physiological effects (e.g. respiration) and changing posture cause PTT and PEP not to be constant. All these effects modulate the PPG signal morphology, fiducial points and, ultimately, PRV. In this sense, this work compares the immunity of chosen fiducial points to the changes in PPG signal morphology with the aim of making the PRV estimate as close to HRV as possible.

Non-invasive optical techniques as PPG can be used to measure blood volume changes using a few opto-electric components. Typically, a red (630–660 nm) or infrared (800–940 nm) light-emitting diode (LED) is used as the light source to illuminate the tissue and a light detector is used to perform PPG measurements in either transmission or reflection mode. In transmission mode, the LED and photodetector (PD) are placed on opposite sides of the tissue and the light passing through it is measured. In reflection mode, the LED and PD are both facing the same side of the tissue and the light backscattered from it is measured. Reflection mode allows measurements from multiple locations on the body while the backscattered light intensity might be significantly lower in comparison with transmission mode measurements. In recent years, several locations for PPG sensors have been explored, such as finger (Rhee *et al* 2001), forehead (Peralta *et al* 2017), earlobe (Lu *et al* 2009, Vescio *et al* 2018), wrist (Grajales *et al* 2006, Salehizadeh *et al* 2015), chest (Chreiteh *et al* 2014) or abdomen (Spigulis *et al* 2005). Wearable pulse rate sensors based on PPG signals have become popular for instantaneous assessment of pulse rate (Tamura *et al* 2014, Zhang *et al* 2014). For clinical purposes, PPG measurements from the earlobe or the forehead can be more suitable and comfortable (Wang *et al* 2007), while ambulatory monitoring systems should be able to detect signals as reliably and stably as possible, such as with finger PPG measurements (Rhee *et al* 2001).

Compared with the ECG signal, the PPG waveform is smooth and not characterized by any clearly detectable features (Rajala *et al* 2017). Hence, an important first step for PRV analysis is accurate detection of the PPG pulse wave and pulse periods (PPs). There is therefore a need to widely define the most accurate fiducial point for performing a PRV analysis under non-stationary conditions based on different PPG morphologies and signal acquisition techniques. Different fiducial points for the temporal location of each pulse wave have been proposed in several studies, such as the apex, middle-amplitude and foot points of the PPG signal, maximum of the first- and second-order derivative PPG signal or the tangent intersection point, depending on the application: from the finger PPG for diagnosis of obstructive sleep apnea (Yao *et al* 2007, Lazaro *et al* 2014), from the earlobe PPG for deriving instantaneous pulse rate (Hemon *et al* 2016) or for measurement of pulse arrival time (Rajala *et al* 2017). Choosing the most feasible sensor location and measurement technique for PRV analysis may thus be challenging (Buxi *et al* 2015).

To the best of our knowledge no study has determined the most suitable and generally accepted PPG measurement technique and fiducial point for accurate pulse detection when exploring the possibility of using the PRV signal to evaluate the ANS. Several studies have investigated and verified the accuracy of PRV as a surrogate of HRV (Porto *et al* 2009, Charlot *et al* 2009, Gil *et al* 2010, Khandoker *et al* 2011) where results show sufficient accuracy under non-stationary conditions, but findings regarding the position of the sensor or the detection algorithm are not conclusive (Schafer *et al* 2013).

The main objective of this paper is to determine the most suitable fiducial point for performing a PRV analysis based on the location of the sensor and the PPG measurement technique in non-stationary conditions. We want to investigate the possibility of using PRV extracted from transmission and reflection PPG signals as a surrogate of HRV and to evaluate the changes in ANS elicited by a tilt-table test. To this end, PPG signals acquired from finger and forehead were considered. Reflection-based PPG signals acquired from the forehead are characterized by smoother shapes, and accurate peak detection of the maximum point of the pulse can be challenging; finger PPG signals may be characterized by a dicrotic notch as the acute drop following the highest single-pulse peak.

2. Materials and methods

2.1. Data and signal pre-processing

ECG and PPG data were simultaneously collected from 18 young healthy subjects (11 females) by the portable device Cardioholter 6.2-8E78 (KTU BMII, Lithuania). The subjects were instructed to avoid substances influencing cardiovascular system activity (e.g. alcohol, caffeine) and smoking for 6 h before the examination. The subjects were normotensive, non-obese and were taking no medication for the duration of the study. Signed, written consent to participate in the study was obtained from all the volunteers, and the ethical principles of the Declaration of Helsinki were followed. Identifiable information was removed from the collected data to ensure participant anonymity. The sampling rates of ECG and PPG signals were 500 Hz and 250 Hz, respectively. For this study, all PPG signals were resampled at $f_s = 500$ Hz. The database includes the conventional three-lead (I, II,

Table 1. Characteristics of the study population: age, height, mass and body mass index.

Age (years)	25.65 ± 2.50
Height (cm)	174.84 ± 9.96
Mass (kg)	67.47 ± 10.67
Body Mass index (kg m^{-2})	21.98 ± 2.27

III) ECG data and four PPG signals at two wavelengths, red (660 nm) and infrared (940 nm), on the finger and on the forehead. A transmission PPG sensor was placed on the right index finger and the reflection PPG sensor above the left eyebrow on the forehead. In this context, with the aim of providing valuable insights to define the best fiducial points for PRV analysis, we carried out a comprehensive evaluation using two wavelengths and five fiducial points per subject ($N = 18 \times 2 \times 5$) for a robust comparison of the variability signals. All subjects underwent a tilt-table test using a Canaletto Pro tilt table (Ferrox S.r.l., Italy), which provokes changes in the ANS. The table was slowly tilted by 80 degrees over 40 s. The protocol consisted of three phases: 10 min in the early supine position (Supine I), 5 min head-up tilt (Tilt) and 5 min back to the supine position (Supine II). Characteristics of the study population are provided in table 1.

The pre-processing stage included automatic QRS detection from the ECG signal using a wavelet-based ECG delineator (Martinez *et al* 2004). Baseline contamination was removed from the PPG using a high-pass filter with a cut-off frequency of 0.3 Hz, and high-frequency noise was attenuated by a low-pass filter with a cut-off frequency of 35 Hz. Zero-phase forward–backward digital filtering was applied in both cases to preserve the pulse morphology.

Artefacts were automatically detected and removed for the variability analysis by an artefact detector based on Hjorth parameters. The algorithm is the result of adapting the algorithm described in Gil *et al* (2008) to non-stationary environments as described in appendix. Additional visual inspection of the finger PPG signals revealed the existence of some noisy PPG segments in the tilted position, most likely due to motion artefacts. Hence, in addition to the artefact detector, artefact segments were identified and excluded from the variability analysis for all signals in the database by visual inspection.

2.2. Fiducial point detection

Five fiducial points were computed and compared to perform PRV analysis: apex (n_A), middle-amplitude (n_M) and foot (n_F) of the PPG pulse, apex (n_A^*) of the derivative PPG signal and intersection point (n_T) of the tangent to the PPG waveform at the apex point n_A^* and the tangent to the PPG waveform at the foot point n_F, defined as the intersecting tangents method. The apex points n_A were detected by an automatic pulse detector developed previously in Lazaro *et al* (2014), which detects the upslope point of each PPG pulse (n_A^*) based on a low-pass differentiator filter and time-varying threshold.

In this paper, in order to better suit the smoother shapes of the reflection-based PPG signals and for greater robustness under non-stationarity conditions, the apex points n_A were set at the maximum point of the PPG pulses within a time window starting at n_{Ai}^*, whose length is half of the median of the three previous instantaneous pulse rate samples ($\hat{m}_{AAi}$):

$$n_{Ai} = \underset{n\epsilon[n_{Ai}^*, n_{Ai}^* + \hat{m}_{AAi}/2]}{\arg\max} \{x(n)\} \tag{1}$$

$$\hat{m}_{AAi} = \text{median}\ (n_{A_{i-4}}^* - n_{A_{i-3}}^*, n_{A_{i-3}}^* - n_{A_{i-2}}^*, n_{A_{i-2}}^* - n_{A_{i-1}}^*) \tag{2}$$

where $x(n)$ corresponds to the PPG signal. Then, the foot points n_F were set as the minimum point of the PPG pulses within a 250 ms window ending at each n_{Ai}^*:

$$n_{Fi} = \underset{n\epsilon[n_{Ai}^* - 0.25 f_s, n_{Ai}^*]}{\arg\min} \{x(n)\}. \tag{3}$$

The middle-amplitude points n_M were set as the point between n_A and n_F where the amplitude has reached half of the maximum of the pulse amplitude:

$$n_{Mi} = \underset{n\epsilon[n_{Fi}, n_{Ai}]}{\arg\min} \left\{ \left| x(n) - \frac{x(n_{Ai}) + x(n_{Fi})}{2} \right| \right\}. \tag{4}$$

Finally, the intersection points n_T of the tangent to the PPG waveform at the apex of the derivative PPG signal n_A^* and the tangent to the foot of the PPG pulse n_F of gradient zero were estimated as described in Hemon *et al* (2016). The five significant points of the ith PPG pulse computed for PRV analysis are shown in figure 1 for both forehead and finger PPG signals, as well as the R waves (n_{Ri}) detected for the ith ECG beat as reference.

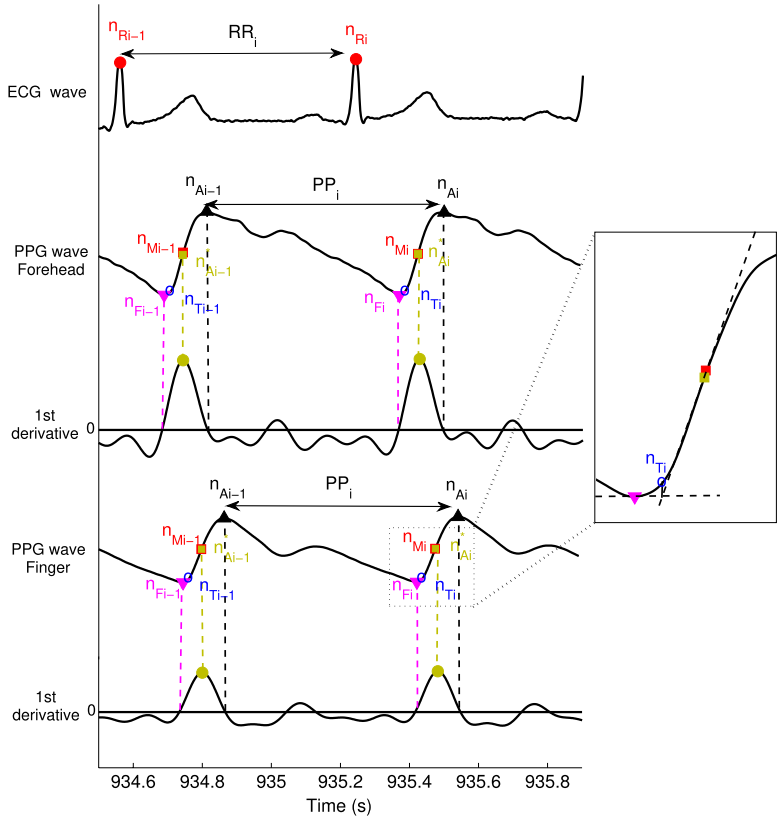

Figure 1. Examples of beat and pulse detection. From top to bottom: R waves detected from the ECG; five fiducial points and first derivative signal obtained from the forehead; five fiducial points and first derivative signal obtained from the finger—apex n_A, middle-amplitude n_M and foot n_F of the pulse amplitude, apex of the first derivative n_A^* and tangent intersection n_T.

2.3. Variability analysis indices

The time difference series between two consecutive R waves from the ECG (RR intervals) and the five fiducial points detected from the PPG (PP intervals) were extracted. Classical time and frequency domain indices from the HRV signal were computed and compared with the indices from the PRV signals. Based on TaskForce (1996), the temporal indices studied in this paper are the mean of heart rate (HRM), the standard deviation of all normal-to-normal intervals (SDNN), the standard deviation of the successive differences of the NN intervals (SDSD), the root mean-square of successive differences of adjacent NN intervals (RMSSD) and the percentage of pairs of adjacent NN intervals differing by more than 50 ms (pNN50). When performing a frequency analysis, the heart and pulse rate oscillations can be divided into two main bands: low frequency (LF; 0.04–0.15 Hz) and high frequency (HF; 0.15–0.4 Hz).

The instantaneous pulse rate signal, $x_{PR}(n)$, was obtained from the different pulse time series using a generalization of the integral pulse frequency modulation model and spline interpolation (Mateo *et al* 2003). Ectopic beats, missed beats and false detections were identified and corrected (Mateo *et al* 2003). Then, the signal $x_{PRM}(n)$ is defined as an estimation of the time-varying mean pulse rate by low-pass filtering the $x_{PR}(n)$ signal with a cut-off frequency of 0.03 Hz. Finally, the variability signals are defined as the difference:

$$x_{PRV}(n) = x_{PR}(n) - x_{PRM}(n). \tag{5}$$

Welch's method (Welch *et al* 1967) was applied to estimate the power spectral density (PSD) of the $x_{PRV}(n)$ signal using a Hamming window of length 42 s with 50% overlap (McNames *et al* 2006). The power at each band of interest, P_{LF} and P_{HF}, was computed from the PSD and the $R_{LF/HF}$ ratio and normalized values (P_{LFn} and P_{HFn}) were estimated. A similar procedure was performed to obtain the $x_{HRV}(n)$ signal and related HRV indices.

2.4. Performance evaluation

In each phase of the protocol, HRV and PRV indices were calculated in short segments with a length in the range of 1–2 min due to the nature of the study (McNames *et al* 2006, Salahuddin *et al* 2007, Baek *et al* 2015, Pecchia *et al* 2018); stationarity is assumed and a valid segment is considered to be one where there are no artefacts during at least 1 min of PPG signal. Otherwise, that segment is discarded for the variability analysis from all signals in the database. The relative error (RE) made in the PRV estimation is calculated for each kth segment and each variability index (I_{PRV} and I_{HRV} for PRV and HRV, respectively) using the HRV signal as reference:

$$E_r(k) = 100 \times \frac{I_{PRV}(k) - I_{HRV}(k)}{I_{HRV}(k)} \qquad k = 1...K, \tag{6}$$

where I is HRM, SDNN, SDSD, RMSSD, pNN50, P_{LF} and P_{HF}.

As a result of this study, the REs in terms of median and interquartile range are presented for each variability index among the available segments for all subjects in the database. Absolute errors are presented for the normalized low-frequency power, P_{LFn} ($P_{HFn} = 1 - P_{LFn}$) and the $R_{LF/HF}$ ratio. These results are separately analyzed for each phase (Supine I, Tilt and Supine II).

The agreement between the RR and PP series was assessed using a Bland–Altman plot (Bland *et al* 1986), where the ECG signal is considered as the gold standard. The bias or average of all differences, the standard deviation around the bias (std) and the limits of agreement (LOA) defined as bias $\pm 1.96\times$ std values were computed for each fiducial point.

The data distribution of HRV and PRV parameters was found by the Kolmogorov–Smirnov test not to be normal, and therefore the non-parametric Wilcoxon and Friedman tests were applied. Bonferroni correction for multiple statistical tests between the five fiducial points was used to reduce the chances of obtaining false-positive results. In this context, four methods were considered for studying the reliability and agreement between HRV and PRV signals:

(i) Pearson's correlation coefficient (ρ) was used to measure the linear strength between the variability indices derived from HRV and PRV signals.
(ii) Two reliability indices were used to measure the interchangeability between measures: Lin's concordance correlation coefficient (CCC; see Lin *et al* (1989)) and the intraclass correlation coefficient (ICC; see Fisher *et al* (1925)) .
(iii) The Wilcoxon paired-test with Bonferroni correction was used to quantify statistical significance and the differences between PRV and HRV signals for the main spectral components within all fiducial points. Then, a second Wilcoxon paired statistical test was performed to evaluate changes in the activity of the ANS during the head-up position with respect to the resting position for ECG and PPG signals. In addition, Cliff's delta statistics for a non-parametric effect size measure are presented.
(iv) Finally, a test using Friedman statistics with Bonferroni multiple comparison was applied to assess the differences between the estimated REs of the five fiducial points.

3. Results

Forehead and finger PPG signals were recorded at two wavelengths, red and infrared. Lower REs between HRV and PRV signals were observed for infrared measurements among all fiducial points, especially during the tilted position. Besides, greater differences were found between both wavelengths in the forehead than in the finger PPG. For instance, the REs estimated during the supine position for infrared versus red recordings in the forehead PPG were, respectively (median/IQR): 18.97/65.90% versus 72.53/157.09% (n_A), 8.48/15.45% versus 17.29/28.57% (n_F), 2.86/4.59% versus 5.33/10.02% (n_M) for the RMSSD index or 6.26/39.43% versus 53.88/299.90 % (n_A), 16.09/17.29% versus 23.23/44.68 % (n_F), 6.84/13.23% versus 6.59/15.37 % (n_M) for P_{HF}. These results suggest that infrared PPG signals are more suitable than red PPG signals for these data. Thus, in the rest of the discussion we focus our analysis on determining the most suitable fiducial point for PRV analysis in the infrared-recorded PPG signals and just those results are presented.

Tables 2 and 3 show the REs obtained in the estimation of the time and frequency domain indices derived during the tilt-table test for the five fiducial points. Results from finger and forehead PPG are compared to assess the changes in the ANS using HRV indices as a reference. These results were obtained by averaging among all subjects the indices presented in section 2.3 in three phases: early supine (Supine I), Tilt and late supine (Supine II). Comparing the results obtained for each fiducial point, higher REs in all indices were observed using n_A and n_F, which are more prominent in the tilted position. The average percentage of discarded signals during the performance of the PRV analysis was roughly 15–20% for all PPG signals. More specifically, the artefact presence per phase (Supine I, Tilt and Supine II) was, respectively, 11.9%, 19.3% and 20% in the forehead and 16.33%, 24.67% and 20% in the finger.

Figure 2 shows Bland–Altman plots that evaluate the discrepancies between RR series obtained from the ECG and all PP series obtained from PPG measurements and the stability across a wider range of values. The central, upper and lower horizontal dashed lines show the bias (mean) and the LOA (bias $\pm$ 1.96 $\times$ std values) of the differences between methods, respectively. Exact values of bias, standard deviation and LOA are shown at the top of each figure, where a total of 26 361 paired RR and PP measurements were used for the analysis. For n_A the discrepancies are higher, in general, for the measurements in the finger.

Table 2. Time domain PRV analysis. Estimated relative errors between HRV and both PRV signal indices (%). Results shown as median/interquartile range values were obtained within all available signal segments for all subjects in the tilt-table test database and for each phase: Supine I, Tilt and Supine II.

		Apex (n_A)		Foot (n_F)		Middle-amplitude (n_M)		First derivative apex (n_A^*)		Tangent intersection (n_T)	
		Forehead	Finger	Forehead	Finger	Forehead	Finger	Forehead	Finger	Forehead	Finger
Supine I	HRM	−0.007/0.20	0.004/0.09	0.005/0.05	0.008/0.05	**0.004/0.07**	0.007/0.041	0.0088/0.06	**0.0041/0.10**	0.006/0.05	0.58/0.07
	SDNN	5.26/11.32	3.82/7.39	2.85/3.01	2.52/1.95	**1.86/2.08**	1.90/2.09	2.78/2.27	**1.77/2.74**	2.80/2.64	2.43/6.71
	SDSD	18.97/65.97	7.98/27.11	8.48/15.46	5.83/5.70	**2.86/4.58**	**3.17/4.43**	3.90/4.28	4.42/2.69	6.21/10.84	4.40/7.53
	RMSSD	18.97/65.90	7.98/27.12	8.48/15.45	5.81/5.68	**2.86/4.59**	**3.11/4.42**	3.90/4.28	4.40/2.70	6.21/10.85	4.40/7.55
	pNN50	8.53/57.39	4.57/19.72	7.80/10.42	3.70/7.86	**0.044/6.16**	**1.49/4.63**	3.26/3.34	2.83/3.51	5.51/6.88	3.23/5.86
Tilt	HRM	−0.017/0.50	−0.14/1.03	**0.001/0.24**	−0.17/0.49	0.024/0.12	−0.22/0.95	0.016/0.27	**0.004/0.42**	0.08/0.20	0.040/0.9
	SDNN	6.65/24.47	4.39/12.31	3.64/5.93	9.54/15.39	**3.37/3.75**	**− 0.59/11.04**	3.59/4.07	0.78/10.83	3.62/5.36	3.34/24.31
	SDSD	64.33/127.70	31.90/47.91	17.55/34.93	54.31/130.03	**5.97/18.82**	12.91/17.42	8.23/16.78	**12.21/11.19**	10.89/26.85	14.11/38.97
	RMSSD	64.06/126.89	31.92/47.77	17.08/34.88	54.23/129.76	**5.96/18.80**	12.91/17.36	8.22/16.77	**12.23/11.15**	10.89/26.85	14.11/38.97
	pNN50	27.87/78.00	14.78/13.83	6.45/16.37	31.63/57.07	**2.88/6.09**	**3.24/6.11**	3.26/4.36	4.20/6.34	3.85/8.36	10.42/20.64
Supine II	HRM	−0.065/0.75	−0.03/0.40	**− 0.001/0.14**	−0.0204/0.62	−0.009/0.22	**− 0.001/0.57**	0.0029/0.33	−0.24/0.60	0.002/0.18	−0.10/0.62
	SDNN	5.19/12.24	0.40/4.54	2.17/3.09	2.92/7.36	**0.88/5.13**	**2.04/3.84**	2.26/2.94	2.54/3.38	2.01/3.26	2.51/3.45
	SDSD	22.84/107.76	12.24/22.66	11.92/15.68	13.78/19.70	**7.30/9.53**	**7.67/11.24**	7.33/6.75	10.33/8.45	8.62/10.21	10.88/15.36
	RMSSD	22.85/107.62	12.20/22.71	11.94/15.63	13.73/19.64	**7.29/9.59**	**7.68/11.22**	7.33/6.77	10.30/8.45	8.62/10.21	10.87/15.36
	pNN50	18.21/49.61	6.04/11.14	4.91/7.45	5.65/13.60	**1.94/5.21**	**2.13/6.84**	3.79/6.30	4.17/5.37	4.36/6.75	4.23/6.13

* The minimum errors obtained for each variability index in the forehead and in the finger within all fiducial points are shown in bold.

Table 3. Frequency domain PRV analysis. Estimated relative (P_{LF}, P_{HF}) and absolute (P_{LF_n}, $R_{LF/HF}$) errors between HRV and both PRV signal indices (%). Results shown as median/interquartile range values were obtained within all available signal segments for all subjects of the tilt-table test database and for each phase: Supine I, Tilt and Supine II.

		Apex (n_A)		Foot (n_F)		Middle-amplitude (n_M)		First derivative apex (n_A^*)		Tangent intersection (n_T)	
		Forehead	Finger	Forehead	Finger	Forehead	Finger	Forehead	Finger	Forehead	Finger
Supine I	P_{LF}	4.32/22.84	7.33/25.50	**4.06/9.76**	6.17/7.44	5.27/7.95	**5.88/7.87**	5.45/9.42	6.84/4.91	6.35/12.15	6.65/4.14
	P_{HF}	6.26/39.43	16.57 /173.80	16.09/17.29	15.54/25.03	6.84/13.23	7.08/12.50	12.71/12.86	11.80/11.63	14.65/16.76	12.47/23.79
	P_{LF_n}	−0.10/1.84	−0.07 /0.74	−0.26/0.82	**− 0.05/0.73**	**− 0.06/0.49**	−0.08/0.44	−0.24/0.49	−0.08/0.39	−0.24/0.57	−0.07/0.46
	$R_{LF/HF}$	−0.11/2.02	−0.07/0.80	−0.27/0.91	−0.05/0.81	−0.07/0.53	−0.09/0.46	−0.26/0.55	−0.08/0.42	−0.26/0.63	−0.07/0.52
Tilt	P_{LF}	15.08/14.90	2.55/58.41	**5.07/15.14**	18.47/396.46	9.60/11.68	**2.18/23.54**	13.60/14.84	5.75/43.19	12.55/14.81	10.61/79.01
	P_{HF}	62.08/156.67	71.76/49.28	36.69/82.76	132.82/744.64	**23.35/37.07**	23.56/30.10	38.87/24.61	**22.86/27.45**	34.82/79.83	39.12/217.42
	P_{LF_n}	−9.52/11.38	−5.49/8.81	−3.91/5.69	−4.44/10.41	−1.50/2.05	**− 2.67/8.54**	**− 1.31/2.96**	−3.77/7.34	−1.98/3.66	−3.95/8.14
	$R_{LF/HF}$	−12.49/14.58	−7.00/11.00	−4.47/9.07	−5.28/14.90	−1.92/3.61	**− 4.26/12.94**	**− 1.77/5.07**	−4.77/9.83	−2.37/6.17	−4.90/11.43
Supine II	P_{LF}	5.05/48.87	4.43/26.38	**1.84/17.28**	4.62/17.35	1.89/17.94	3.23/10.34	9.79/30.74	**2.36/25.03**	5.32/21.05	4.28/18.49
	P_{HF}	29.51 /213.42	20.33/73.77	30.85/37.48	25.85/58.94	6.56/53.70	9.39/24.89	18.78/44.96	14.67/36.12	23.91/39.28	21.96/49.53
	P_{LF_n}	−0.09/2.53	−0.02/1.22	−0.28/1.53	−0.40/1.49	**− 0.09/1.29**	**− 0.084/0.96**	−0.22/0.90	−0.09/1.11	−0.24/1.06	−0.22/1.23
	$R_{LF/HF}$	−0.09/2.63	−0.02/1.30	−0.28/1.71	−0.41/1.68	**− 0.09/1.40**	**− 0.08/1.04**	−0.23/1.03	−0.09/1.17	−0.24/1.19	−0.29/1.40

* The minimum errors obtained for each variability index in the forehead and in the finger within all fiducial points are shown in bold.

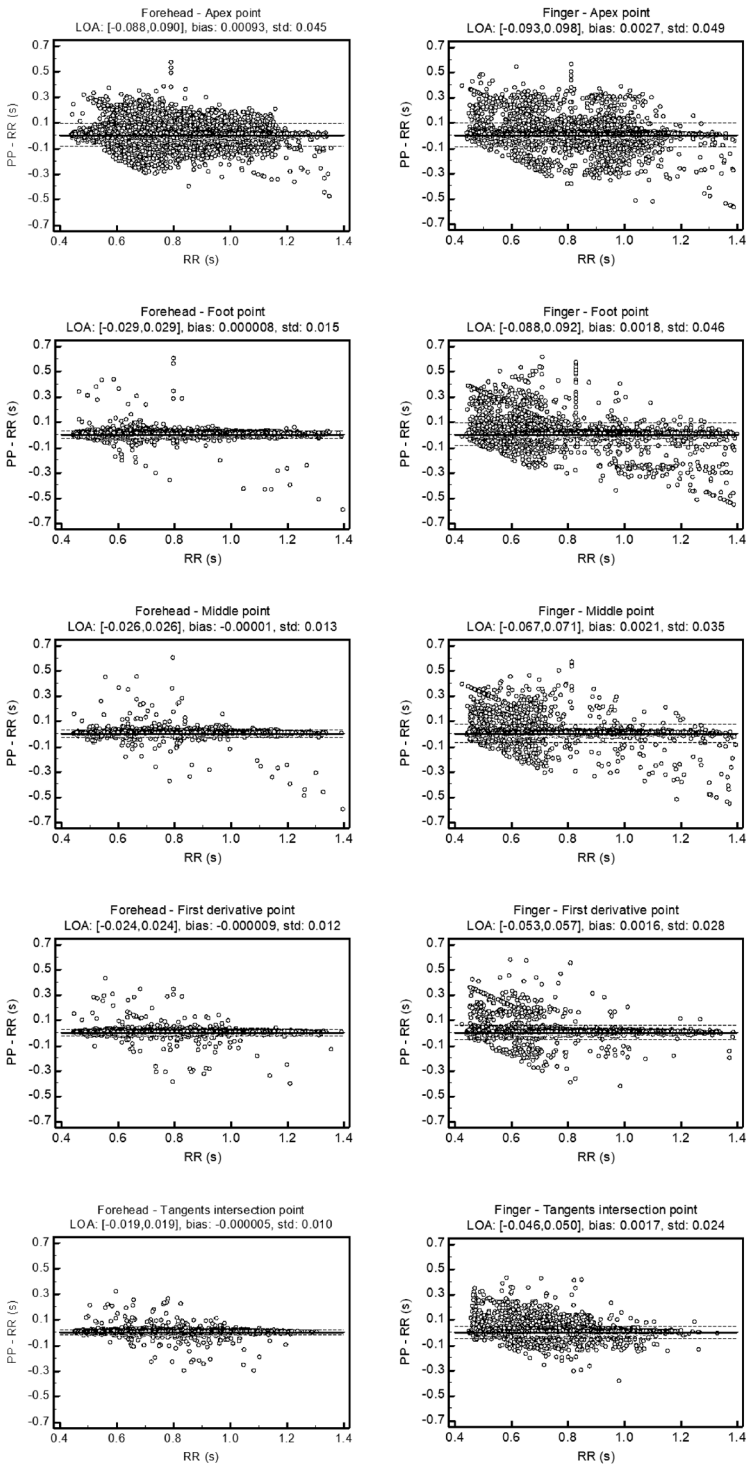

Figure 2. Bland–Altman plots comparing paired RR and PP series obtained from forehead (right) and finger (left) PPG signals within all fiducial points for all subjects. Bias and limits of agreement (bias $\pm$ 1.96 $\times$ std values) are shown by solid and dashed lines, respectively.

Pearson's correlation between HRV and PRV signals was quantified for P_{LF} and P_{HF}. Significant and positive linear correlation ($\rho > 0.9$) was found in both indices for the tilted position using n_F, n_M, n_A^* and n_T for the forehead PPG and using n_M, n_A^* and n_T for the finger PPG as shown in table 4. In addition, we consider CCC and ICC coefficient values lower than 0.7 as markers of poor reliability between HRV and PRV signals. In this sense, n_A in the forehead or n_A and n_F in the finger provide the lowest values.

Statistically significant differences were found between HRV and PRV signals in the tilted position according to the Wilcoxon paired test as shown in figure 3, using the Bonferroni correction for multiple comparisons. In particular, significant differences (p-value < 0.01) were found in P_{HF} between forehead PRV and HRV using n_A and between finger PRV and HRV using n_A, n_F and n_T.

Table 4. Pearson's correlation (ρ) and reliability coefficients (CCC, ICC) between HRV and PRV signals for P_{LF}, P_{HF} and for each phase: Supine I, Tilt and Supine II.

			Forehead					Finger				
			n_A	n_F	n_M	n_A^*	n_T	n_A	n_F	n_M	n_A^*	n_T
Supine I	P_{LF}											
		ρ	**0.96**	**0.99**	**0.99**	**0.99**	**0.99**	**0.95**	**0.99**	**0.99**	**0.99**	**0.98**
		CCC	**0.94**	**0.99**	**0.99**	**0.99**	**0.99**	**0.94**	**0.99**	**0.99**	**0.99**	**0.99**
		ICC	**0.97**	**0.99**	**0.99**	**0.99**	**0.99**	**0.97**	**0.99**	**0.99**	**0.99**	**0.99**
	P_{HF}											
		ρ	0.85	**0.99**	**0.99**	**0.99**	**0.99**	**0.920**	**0.99**	**0.99**	**0.99**	**0.99**
		CCC	0.78	**0.98**	**0.99**	**0.99**	**0.99**	0.89	**0.99**	**0.99**	**0.99**	**0.99**
		ICC	0.88	**0.99**	**0.99**	**0.99**	**0.99**	**0.95**	**0.99**	**0.99**	**0.99**	**0.99**
Tilt	P_{LF}											
		ρ	0.82	**0.98**	**0.98**	**0.99**	**0.99**	**0.96**	0.36	**0.93**	0.78	0.77
		CCC	0.79	**0.96**	**0.95**	**0.96**	**0.97**	**0.95**	0.10	**0.91**	0.77	0.70
		ICC	0.89	**0.98**	**0.98**	**0.98**	**0.98**	**0.98**	0.06	**0.96**	0.88	0.86
	P_{HF}											
		ρ	−0.06	**0.96**	**0.98**	**0.99**	**0.99**	0.66	**0.92**	**0.90**	**0.91**	**0.92**
		CCC	−0.09	0.64	0.88	**0.91**	0.85	0.46	0.004	0.80	0.83	0.86
		ICC	−0.15	0.78	**0.93**	**0.95**	**0.93**	0.58	0.004	0.89	**0.91**	**0.92**
Supine II	P_{LF}											
		ρ	**0.96**	**0.98**	**0.98**	**0.98**	**0.98**	**0.97**	**0.90**	**0.97**	**0.95**	**0.94**
		CCC	**0.95**	**0.96**	**0.95**	**0.96**	**0.96**	**0.97**	0.53	**0.93**	0.74	0.70
		ICC	**0.97**	**0.98**	**0.97**	**0.98**	**0.98**	**0.98**	0.70	**0.96**	0.85	0.81
	P_{HF}											
		ρ	0.89	**0.92**	**0.98**	**0.97**	**0.93**	**0.90**	**0.90**	**0.95**	**0.99**	**0.98**
		CCC	0.85	0.88	**0.98**	**0.94**	**0.91**	0.87	0.86	**0.94**	**0.98**	**0.97**
		ICC	**0.92**	**0.93**	**0.99**	**0.97**	**0.94**	**0.93**	**0.93**	**0.97**	**0.99**	**0.99**

* Values higher than 0.9 are shown in bold.

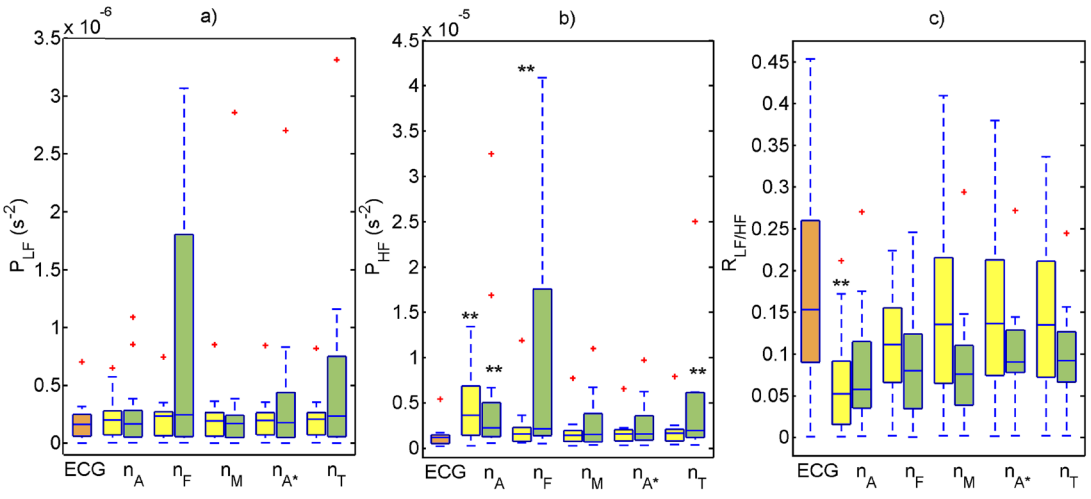

Figure 3. Inter-subject medians of (a) P_{LF}, (b) P_{HF} and (c) $R_{LF/HF}$ ratios from ECG (orange bars), forehead PPG (yellow bars) and finger PPG (green bars) for each fiducial point in the head-up tilted position. The outliers are plotted individually using red markers ('+'). Significant differences (p-value < 0.01) according to the Wilcoxon paired statistical test are denoted between compared groups (ECG/forehead and ECG/finger) with (**).

In the head-up tilted position, the REs are significantly higher in P_{HF} using n_A in the forehead and in P_{LF} and P_{HF} using n_F in the finger compared with the n_M and n_A^* fiducial points according to the Friedman statistics with Bonferroni multiple comparison (see figure 4). In addition, during early and late supine stages it can be observed that the REs in P_{HF} are significantly lower using n_M compared with other fiducial points.

Results of the Wilcoxon paired test comparing changes in ANS activity in the head-up position with respect to the resting position are presented in table 5 for the pairs Supine I/Tilt and Supine II/Tilt. It was observed that HRV

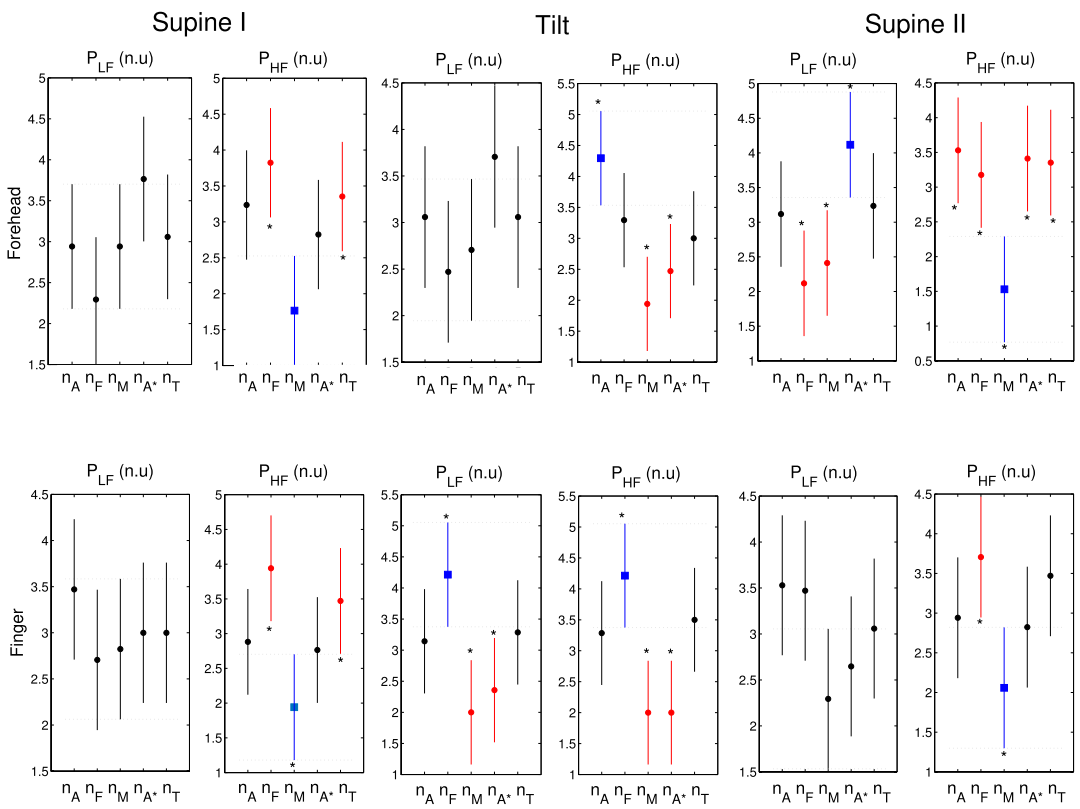

Figure 4. Mean values of relative errors of P_{LF} and P_{HF} obtained in the estimation of PRV indices using HRV as a reference. Results are shown for each fiducial point during early supine, tilt and late supine stages in the forehead (top) and finger (bottom) PPG signals. The asterisk (*) indicates statistically significant differences between compared groups using Friedman statistics with the Bonferroni multiple-comparison test when the mean value of one fiducial point (blue) is significantly higher or lower than other(s) (red).

Table 5. The p-value obtained by the Wilcoxon paired test between compared pairs (Supine I/Tilt and Supine II/Tilt) for ECG and both PPG signals. The effect size is shown in brackets.

		ECG		Forehead		Finger	
		SupI/Tilt	SupII/Tilt	SupI/Tilt	SupII/Tilt	SupI/Tilt	SupII/Tilt
n_M	P_{LF}	**0.032** (0.43)	0.062 (0.37)	**0.030** (0.43)	0.085 (0.34)	**0.023** (0.30)	**0.042** (0.27)
	P_{HF}	0.091 (0.34)	**0.023** (0.46)	0.28 (0.21)	**0.042** (0.41)	0.37 (0.20)	0.26 (0.25)
	$R_{LF/HF}$	**0.001** (0.64)	**0.002** (0.60)	**0.001** (0.66)	**0.003** (0.58)	**0.009** (0.59)	**0.005** (0.56)
n_A^*	P_{LF}	**0.032** (0.39)	0.062 (0.38)	**0.038** (0.41)	0.053 (0.39)	**0.021** (0.30)	**0.042** (0.27)
	P_{HF}	0.091 (0.34)	**0.023** (0.44)	0.17 (0.28)	**0.023** (0.46)	0.32 (0.22)	0.175 (0.30)
	$R_{LF/HF}$	**0.001** (0.64)	**0.002** (0.60)	**0.001** (0.68)	**0.001** (0.63)	**0.002** (0.64)	**0.003**(0.54)

* p-values lower than 0.05 are shown in bold.

and PRV signals give similar results using n_M and n_A^* but not for the rest, so only the results for those fiducial points are presented. Besides, large effect sizes (ES) show that differences in HRV or PRV between the phases of the tilt-table test are more important than the differences between HRV and PRV signals (ES < 0.1 in P_{LF} and ES < 0.2 in P_{HF} in the supine position or ES < 0.20 in P_{LF} and ES < 0.30 in P_{HF} using n_M, n_A^* and n_T in the tilted position).

4. Discussion

In this work we analyze the most accurate fiducial points for PRV analysis as a surrogate for HRV under non-stationary conditions in young healthy subjects. For this purpose, five fiducial points were computed and their suitability for PRV analysis was compared based on the location of the sensor, forehead or finger, and two PPG measurement techniques, reflection or transmission mode. First, the classical time and frequency variability indices were estimated for each fiducial point in the three phases of the tilt table test. In order to measure P_{LF} and P_{HF}, at least 1 min of HRV and PRV signals is needed (Pecchia *et al* 2018). Therefore, due to the nature of this

study, the length of the segments and the Hamming window were chosen to provide a reliable estimation of the power P_{LF} (McNames *et al* 2006, Baek *et al* 2015) and an accurate comparison between the variability signals. Second, statistical differences are quantified between PRV and HRV indices within each fiducial point and to evaluate changes in the ANS provoked during the tilt-table test with respect to baseline conditions.

Several studies have indicated differences that are sufficiently small to suggest the use of PRV as an alternative measurement of HRV (Gil *et al* 2010, Khandoker *et al* 2011). It has been pointed out that PRV can be used to discriminate sleep apneic and non-apneic decreases in the amplitude fluctuations of the PPG signal without introducing any additional signal, for example ECG (Lazaro *et al* 2014). Hence, PPG signals are especially relevant in sleep studies because there is no need to use many sensors which could disturb physiological sleep.

Our results suggest that infrared PPG signals are more suitable than red PPG signals in these data. However, the wavelength of light used affects the quality of the acquired PPG signal in several ways. On one hand, the interaction of hemoglobin with the light depends on the wavelength. Most of the hemoglobin in arteries is oxygenated and the absorption coefficient of oxygenated hemoglobin in infrared is higher than in red light. Therefore, the AC component of the infrared PPG signal is expected to have a higher dynamic range, which may reduce the error in location of fiducial points, making an infrared PPG signal more convenient than a red one. On the other hand, shorter wavelengths have shorter penetration than the longer wavelengths, leading to measures that are more affected by the local tissues and less corrupted by the ambient light. However, the light has to penetrate deep enough to interact with arterial vessels, so too short a wavelength is not convenient either. Furthermore, melanin has a huge interaction with light, making the optimal choice of wavelength dependent on the type of the skin of the subject. The superposition of all these effects leads to higher signal quality using red or infrared and, in this case, our observation is that infrared is more convenient than red, in agreement with Fallow *et al* (2013), where infrared PPG signals are reported to have a higher signal-to-noise ratio than red PPG signals when measuring on subjects with white skin.

4.1. Variability estimation accuracy

The accuracy of the PRV estimation is very dependent on the technique used to acquire the signal, the possible signal interferences or artefacts and the morphology of the PPG signal according to the recording methodology and location of the sensor on the body. In line with other studies (Schafer *et al* 2013, Peng *et al* 2015), our results show higher REs between PRV and HRV for RMSSD or SDSD variability indices than for SDNN. Also, low-frequency indices are better aligned than high-frequency indices between both variability signals (Gil *et al* 2010).

4.1.1. Time domain

Time domain indices derived from forehead and finger PRV signals present a small RE in the supine position, with values lower than 8%, 10% and 11% for fiducial points n_M, n_A^* and n_T, respectively. It has been shown that for indices related to short-term variability, such as SDSD and RMSSD, the REs are higher in the tilted position than during the supine interval, with values lower than 15% for these three fiducial points. Moreover, it should be noted that higher REs are obtained for n_A and n_F in both supine and tilted positions. The global results suggest that PRV analysis could be used as a surrogate measurement for HRV analysis especially with the forehead PPG signals, with REs of 6%, 8% and 11% (n_M, n_A^* and n_T) compared with 12%, 13% and 14% with finger PPG signals.

4.1.2. Frequency domain

Frequency domain indices derived from both PRV signals present REs lower than 25% in the supine position in P_{LF} and P_{HF}, with values lower than 6%, 10% or 7% in P_{LF} and 10%, 19% or 24% in P_{HF} for n_M, n_A^* and n_T fiducial points, respectively. The REs have a higher variance in the head-up position, especially for the P_{HF} and $R_{LF/HF}$ ratio. For instance, for finger PPG signals values (median/IQR) are 2/23%, 6/43% and 10/80% (n_M, n_A^* and n_T) in P_{LF} and 24/30%, 23/27% and 40/217% in P_{HF} compared with 10/11%, 13/14% and 13/15% in P_{LF} and 24/37%, 39/25% and 35/80% in P_{HF} for forehead PPG. Due to the small values obtained in P_{HF} for the reference HRV, the REs for HF-related indices in the head-up position could be higher than expected according to the RE estimation defined in equation 6. In line with the results for the time domain-related indices, higher REs are observed for n_A and n_F in supine and tilted positions.

In general, the REs are slightly lower for the reflection-based PPG signals measured in the forehead than for the transmission-based PPG signals measured in the finger, in particular in the head-up position. One of the most important limitations of PPG signals for PRV analysis is motion artefacts. The effect of motion artefacts was investigated during this study: approximately 15% of the forehead PPG signals were considered to be artefacts and were discarded for the PRV analysis while 20% of the finger PPG signals were discarded. This analysis suggests that forehead PRV signals could provide more reliable information under non-stationary conditions while finger PRV signals may be more affected by motion artefacts.

4.2. Statistical analysis

The Bland–Altman plots between RR and PP series exhibited close agreement between measures, the estimated bias being below 0.002 for all cases. The analysis shows a larger divergence in the finger than in the forehead measurements. More specifically, the limits of agreement in the forehead were below [−0.03,0.03] for n_M, n_A^* and n_T. Pearson's correlation between HRV and both PRV signals show a significant and positive linear relationship ($\rho > 0.9$) during the early supine stage for all fiducial points except n_A in the forehead PPG. Besides, strong correlation in the tilted position is observed for all fiducial points except n_A between HRV and forehead PRV indices and for n_M, n_A^* and n_T between HRV and finger PRV. Weaker correlation coefficients as well as higher REs presented in tables 2 and 3 suggest that n_A is not an accurate feature for PRV analysis in the forehead, as it is located at smooth zones of the PPG morphology and its location can be affected by a low level of noise.

The Wilcoxon paired-test using the Bonferroni correction was performed to corroborate our assumptions. No statistically significant differences were found in the early or late supine positions between HRV and PRV signals in the finger and in the forehead. Figure 3 shows that statistically significant differences (p-value < 0.01) were found between PRV and HRV signals for the pair ECG/finger using n_A, n_F and n_T in the head-up position in P_{HF}, and for the pair ECG/forehead using n_A. It is well known that accurate pulse detection is crucial in PRV analysis, thus these results suggest that the apex and foot points of the PPG pulse are less accurate for PRV analysis than the other PPG morphologies.

In order to verify which fiducial point would be more suitable for PRV analysis, statistically significant differences between compared groups were analyzed by using Friedman statistics with the Bonferroni multiple-comparison test. During early and late supine stages, the REs in P_{HF} are significantly lower for n_M compared with n_F and n_T (figure 4), with REs of 6% compared with 20% or 30% as shown in table 3 for Supine II. On the other hand, significantly higher errors during tilting in P_{HF} are observed for n_A in the forehead PPG as well as in P_{LF} and P_{HF} for n_F in the finger PPG compared with n_M and n_A^*. These results confirm that the apex and foot points of the PPG pulse seem to be less accurate for a PRV analysis, with the lowest-reliability indices and wider LOA in n_A for the forehead PPG and in n_F for the finger PPG. Strong correlation (ICC > 0.9) and a narrower LOA indicate that the PP series obtained from the middle-amplitude point and the apex point of the first derivative are interchangeable with the RR series for performing a variability analysis.

Finally, a second Wilcoxon test was performed to evaluate changes in ANS activity in the tilted position with respect to baseline conditions for ECG and PPG signals. It is shown that there are statistically significant differences between the pairs Supine I/Tilt in P_{LF} and Supine II/Tilt in P_{HF}. It should be noted that HRV and forehead PRV signals present similar results using n_M and n_A^* fiducial points, therefore the same physiological interpretation of HRV and PRV can be assumed. In addition, HRV and finger PRV signals present similar results for both fiducial points for the pair Supine I/Tilt but not for the pair Supine II/Tilt in P_{HF}, which could be due to the recovery of the ANS following orthostatic stress. Consequently, PRV could be used to evaluate ANS activity under non-stationary conditions based on the PPG pulses detected in the middle-amplitude point and the apex point of the first derivative.

4.3. Selection of fiducial points

The apex n_A is probably the most common fiducial point used to calculate PP intervals. Its location in the forehead PPG is normally at smooth zones where a low level of noise can significantly change its temporal location. The REs obtained in the PRV indices compared with the HRV ones using the apex n_A are the highest of the five fiducial points presented, and statistically significant differences were found between HRV and both PRV signals. Previously, in figure 1, the smoother shapes of the reflection-based PPG waveforms were analyzed and these results confirm that the apex n_A is not the most suitable point for a PRV analysis due to its limited robustness, especially for forehead PPG signals. The accuracy of the foot point n_F for PPG pulse detection depends on the morphology of the PPG pulse. The REs obtained in the estimation of PRV indices in the tilt position for this point are higher than for other fiducial points and, in particular, for the transmission-based PPG signals in the finger. The results presented in tables 2 and 3 show that the middle-amplitude point n_M, the apex point of the first derivative n_A^* and the tangent intersection point n_T are the most suitable fiducial points for a PRV analysis, particularly in the head-up tilted position related to sympathetic activation of the ANS. The middle-amplitude point of the AC component of the PPG signal, n_M, is located at the systolic slope of the PPG pulse, which is an abrupt zone and is therefore more robust against noise in all kinds of PPG morphologies. This point is measured from the PPG signal itself and it is computationally efficient. The PPG derivative signal is characterized by a sharp and well-defined peak n_A^* above the noise floor, which is again easy to detect. However, its physiological interpretation and temporal relation to the ECG signal could be more difficult to analyze. The intersecting method, which defines n_T, is the most computationally demanding method. It depends on two other fiducial points (n_F and n_A^*) and the inaccurate detection of one point could be compensated by the other.

In accordance with our results, in Rajala *et al* (2017) the apex point of the first derivative was considered the most promising fiducial point for use in pulse arrival time while in Hemon *et al* (2016) for ear PPG and Posada-

Quintero *et al* (2013) for finger PPG the correlation between PPG and ECG for a PRV analysis under stationary conditions was greatest for the intersecting tangents method followed by the apex of the first derivative. To the best of our knowledge, no previous studies have defined the most accurate fiducial point for performing a PRV analysis under non stationary-conditions or have considered the possible impact of artefacts for different PPG morphologies. Based on our results, n_M, n_A^* and n_T can be used for PRV analysis, and we propose the middle-amplitude point of the PPG as the most accurate one under different PPG morphologies and sensor locations, obtaining statistically significant lower REs in P_{LF} and P_{HF} within all fiducial points as shown in figure 4 and in tables 2 and 3.

4.4. Limitations

One potential limitation of this study is the fact that our database consists of mostly young, healthy individuals. Due to the limited number of subjects in the database and the major presence of artefacts in the transmission-based PPG signals acquired from the finger, a further study should validate the suitability of forehead and finger PPG signals for PRV analysis in a comprehensive sample set. Second, the signals in this study were acquired in a well-controlled experiment and motion artefacts were substantially suppressed. In real scenarios, motion artefacts can be more disturbing. In addition, the transmission PPG sensor was placed on the right index finger in this study. According to Yeragani *et al* (2007), there was no significant difference between the right and left sides of the body for measurement of PPG signals in normal controls. However, this would be an interesting point to address in a future work.

5. Conclusion

The middle-amplitude point, the apex point of the first derivative and the tangent intersection point variability-related indices have the lowest REs estimated between PRV and HRV indices and the highest correlation and agreement coefficients. Our results indicate that these fiducial points are more suitable for PRV analysis, and we propose the middle-amplitude point of the PPG as the most accurate one under non-stationarity conditions based on two different locations of the sensor, forehead and finger, and two PPG measurement techniques, reflection and transmissions modes, considering the possible impact of the presence of artefacts. This point is one of the most efficient in terms of computation and statistically significantly lower REs were observed in P_{LF} and P_{HF} within all fiducial points.

In general, the REs are lower for forehead PPG than for finger PPG. For physiological interpretation, the changes in ANS activity in the head-up tilted position with respect to the resting position showed similar results between HRV and forehead PRV for the middle-amplitude point and the apex point of the first derivative. These findings suggest that forehead PPG signals could provide more reliable PRV information than finger PPG under non-stationary conditions.

Acknowledgment

This work was partially financed by Ministerio de Economía, Industria y Competitividad (MINECO) and by fondos FEDER through the project RTI2018-097723-B-I00, by Government of Aragon and European Social Fund (EU) through Grupo de Referencia BSICoS (T39 17R), by University of Zaragoza (UZ2018-TEC-05) and by CIBER in Bioengineering, Biomaterials and Nanomedicine (CIBER–BBN) through Instituto de Salud Carlos III. This work was partially supported by the Research Council of Lithuania (agreement no. S-MIP-17/81). This project has received funding from the European Union Framework Programme for Research and Innovation Horizon 2020 (2014–2020) under the Marie Skodowska–Curie Grant Agreement no. 745755. The computation was performed by the Infrastructure for the production and characterization of Nanomaterials, Biomaterials and Systems in Biomedice (ICTS NANBIOSIS), specifically by the High Performance Computing Unit of CIBER-BBN at the University of Zaragoza.

Appendix. Automatic artefact detection

The first Hjorth parameter (H_1) is defined as an estimate of the central frequency of the signal and the second Hjorth parameter (H_2) as half of the bandwidth. For an intra-subject robustness analysis, a median adaptive filter was implemented using a window length of 4 min to define $\widehat{H_1(n)}$ and $\widehat{H_2(n)}$. Empirical thresholds were used to determine whether a signal segment should be considered as an artefact under the following conditions:

$$H_2(n) > \underbrace{\widehat{H_2(n)} + T_2^u}_{\eta_2^u} \parallel H_1(n) > \underbrace{\widehat{H_1(n)} + T_1^u}_{\eta_1^u} \parallel H_1(n) < \underbrace{\widehat{H_1(n)} - T_1^l}_{\eta_1^l} \tag{A.1}$$

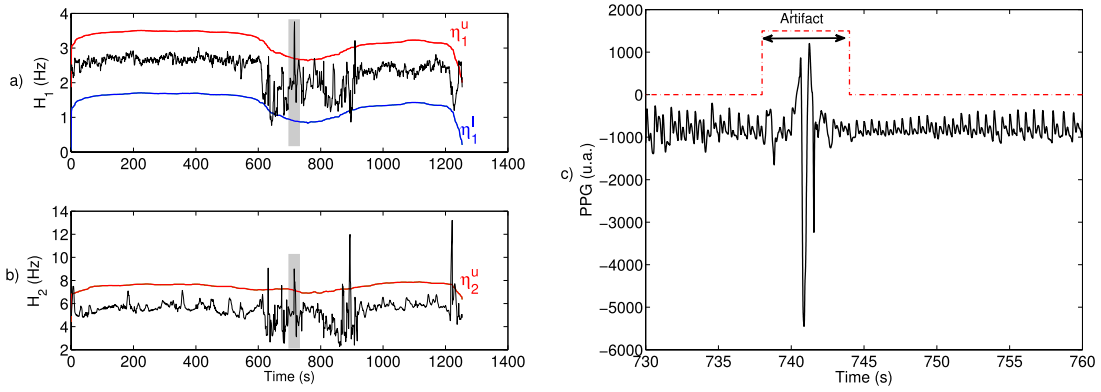

Figure A1. Hjorth parameters, (a) H_1 and (b) H_2, and related thresholds η estimated for one PPG transmission-based signal and (c) one related artefact segment detected within the time interval 730–760 s (shaded area).

where $T_1^u = 1.4$ Hz, $T_1^l = 1$ Hz, $T_2^u = 1.7$ Hz for finger PPG and $T_2^u = 0.8$ Hz for forehead PPG.

The Hjorth parameters estimated for one PPG transmission-based signal are shown in figures A1(a) and (b). As an example of the applicability of the artefact detector, one artefact segment detected is shown in figure A1(c).

References

Allen J *et al* 2007 Photoplethysmography and its application in clinical physiological measurement *Physiol. Meas.* **28** R1

Baek H *et al* 2015 Reliability of ultra-short-term analysis as a surrogate of standard 5 min analysis of heart rate variability *Telemed. e-Health* **21** 404–14

Bernardi L *et al* 1997 Synchronous and baroceptor-sensitive oscillations in skin microcirculation: evidence for central autonomic control *Am. J. Physiol. Heart Circ. Physiol.* **273** 1867–78

Bland J *et al* 1986 Statistical methods for assessing agreement between two methods of clinical measurement *Lancet* **1** 307–10

Buxi D *et al* 2015 A survey on signals and systems in ambulatory blood pressure monitoring using pulse transit time *Physiol. Meas.* **36** R1

Charlot K *et al* 2009 Interchangeability between heart rate and photoplethysmography variabilities during sympathetic stimulations *Physiol. Meas.* **30** 1357

Chreiteh S *et al* 2014 Sternal pulse rate variability compared with heart rate variability on healthy subjects *Conf. Proc. IEEE Engineering in Medicine and Biology Society* pp 3394–7

Fallow B *et al* 2013 Influence of skin type and wavelength on light wave reflectance *J. Clin. Monit. Comput.* **27** 313–7

Fisher R *et al* 1925 *Statistical Methods for Research Workers* (Edinburgh: Oliver & Boyd)

Gil E *et al* 2008 Detection of decreases in the amplitude fluctuation of pulse photoplethysmography signal as indication of obstructive sleep apnea syndrome in children *Biomed. Signal Process. Control* **3** 267–77

Gil E *et al* 2010 Photoplethysmography pulse rate variability as a surrogate measurement of heart rate variability during non-stationary conditions *Physiol. Meas.* **31** 1271

Grajales L *et al* 2006 Wearable multisensor heart rate monitor *Int. Workshop on IEEE Wearable and Implantable Body Sensor Networks* (https://doi.org/10.1109/BSN.2006.58)

Hemon M *et al* 2016 Comparison of foot finding methods for deriving instantaneous pulse rates from photoplethysmographic signals *J. Clin. Monit. Comput.* **30** 157–68

Khandoker A *et al* 2011 Comparison of pulse rate variability with heart rate variability during obstructive sleep apnea *Med. Eng. Phys.* **33** 204–9

Lazaro J *et al* 2014 Pulse rate variability analysis for discrimination of sleep-apnea-related decreases in the amplitude fluctuations of pulse photoplethysmographic signal in children *IEEE J. Biomed. Health Inform.* **18** 240–6

Lin L *et al* 1989 A concordance correlation coefficient to evaluate reproducibility *Biometrics* **45** 255–68

Lu G *et al* 2009 A comparison of photoplethysmography and ECG recording to analyse heart rate variability in healthy subjects *J. Med. Eng. Technol.* **33** 634–41

Martinez J *et al* 2004 A wavelet-based ECG delineator: evaluation on standard databases *IEEE Trans. Biomed. Eng.* **51** 570–81

Mateo J *et al* 2003 Analysis of heart rate variability in the presence of ectopic beats using the heart timing signal *IEEE Trans. Biomed. Eng.* **50** 334–43

McNames J *et al* 2006 Reliability and accuracy of heart rate variability metrics versus ECG segment duration *Med. Biol. Eng. Comput.* **44** 747–56

Niztan M *et al* 1998 The variability of the photoplethysmographic signal—a potential method for the evaluation of the autonomic nervous system *Physiol. Meas.* **19** 93

Pecchia L *et al* 2018 Are ultra-short heart rate variability features good surrogates of short-term ones? State-of-the-art review and recommendations *Healthcare Technol. Lett.* **5** 94–100

Peng R *et al* 2015 Extraction of heart rate variability from smartphone photoplethysmograms *Comput. Math. Methods Med.* (https://doi.org/10.1155/2015/516826)

Peralta E *et al* 2017 Robust pulse rate variability analysis from reflection and transmission photoplethysmographic signals *2017 Computing in Cardiology, IEEE* pp 1–4

Porto L *et al* 2009 Comparison of time-domain short-term heart interval variability analysis using a wrist-worn heart rate monitor and the conventional electrocardiogram *Pacing Clin. Electrophysiol.* **32** 43–51

Posada-Quintero H *et al* 2013 Evaluation of pulse rate variability obtained by the pulse onsets of the photoplethysmographic signal *Physiol. Meas.* **34** 179

Rajala S *et al* 2017 Pulse arrival time (PAT) measurement based on arm ECG and finger PPG signals-comparison of PPG feature detection methods for PAT calculation *39th Annual Int. Conf. of the IEEE Engineering in Medicine and Biology Society* pp 250–3
Rhee S *et al* 2001 Artefact-resistant power-efficient design of finger-ring plethysmographic sensors *IEEE Trans. Biomed. Eng.* **48** 795–805
Salahuddin L *et al* 2007 Ultra short term analysis of heart rate variability for monitoring mental stress in mobile settings *Conf. Proc. IEEE Engineering in Medicine and Biology Society* pp 4656–9
Salehizadeh S *et al* 2015 A novel time-varying spectral filtering algorithm for reconstruction of motion artefact corrupted heart rate signals during intense physical activities using a wearable photoplethysmogram sensor *Sensors* **16** 10
Schafer A *et al* 2013 How accurate is pulse rate variability as an estimate of heart rate variability? *Int. J. Cardiol.* **166** 15–29
Spigulis J *et al* 2005 Optical noninvasive monitoring of skin blood pulsations *Appl. Opt.* **44** 1850–7
Tamura T *et al* 2014 Wearable photoplethysmographic sensors—past and present *Electronics* **3** 282–302
TaskForce 1996 Heart rate variability: standards of measurement, physiological interpretation and clinical use. Task Force of the European Society of Cardiology and the North American Society of Pacing and Electrophysiology *Circulation* **17** 1043–65
Vescio B *et al* 2018 Comparison between electrocardiographic and earlobe pulse photoplethysmographic detection for evaluating heart rate variability in healthy subjects in short- and long-term recordings *Sensors* **18** 844
Wang L *et al* 2007 Multichannel reflective PPG earpiece sensor with passive motion cancellation *IEEE Trans. Biomed. Circuits Syst.* **1** 235–41
Welch P *et al* 1967 The use of fast Fourier transform for the estimation of power spectra: a method based on time averaging over short, modified periodograms *IEEE Trans. Audio Electroacoust.* **15** 70–3
Yao J *et al* 2007 A pilot study on using derivatives of photoplethysmographic signals as a biometric identifier *29th Annual Int. Conf. of the IEEE Engineering in Medicine and Biology Society* pp 4576–9
Yeragani V *et al* 2007 Exaggerated differences in pulse wave velocity between left and right sides among patients with anxiety disorders and cardiovascular disease *Psychosom. Med.* **69** 717–22
Zhang Z *et al* 2014 Troika: a general framework for heart rate monitoring using wrist-type photoplethysmographic signals during intensive physical exercise *IEEE Trans. Biomed. Eng.* **62** 522–31